Computed Radiography Dual Energy Subtraction: Performance Evaluation When Detecting Low-Contrast Lung Nodules in an Anthropomorphic Phantom

Carolyn Kimme-Smith, Donna Lynn Davis, Michael McNitt-Gray, Jonathan Goldin, Eric Hart, Poonam Batra, and Timothy D. Johnson

A dedicated chest computed radiography (CR) system has an option of energy subtraction (ES) acquisition. Two imaging plates, rather than one, are separated by a copper filter to give a high-energy and low-energy image. This study compares the diagnostic accuracy of conventional computed radiography to that of ES obtained with two radiographic techniques. One soft tissue only image was obtained at the conventional CR technique ($\bar{s}$ = 254) and the second was obtained at twice the radiation exposure ($\bar{s}$ = 131) to reduce noise. An anthropomorphic phantom with superimposed low-contrast lung nodules was imaged 53 times for each radiographic technique. Fifteen images had no nodules; 38 images had a total of 90 nodules placed on the phantom. Three chest radiologists read the three sets of images in a receiver operating characteristic (ROC) study. Significant differences in Az were only found between (1) the higher exposure energy subtracted images and the conventional dose energy subtracted images (P = .095, 90% confidence), and (2) the conventional CR and the energy subtracted image obtained at the same technique (P = .024, 98% confidence). As a result of this study, energy subtracted images cannot be substituted for conventional CR images when detecting low-contrast nodules, even when twice the exposure is used to obtain them.

KEY WORDS: lung nodules, computerized radiography, energy subtraction, ROC.

RADIOLOGY DEPARTMENTS that are moving toward a filmless environment by means of a Picture Archiving and Communications System (PACS) often include computed radiography (CR) for many of their plain film examinations.[1-3] Computed radiography is available, as described in these three references, from a variety of manufacturers. High volume chest radiography often uses dedicated CR chest units, like the Fuji FCR 9501 (Fuji Medical Systems; Stanford, CT), because they can eliminate phosphor plate handling with integrated exposure and development functions. This unit also includes an option to provide energy subtraction (ES) images routinely. This algorithm is usually implemented by acquiring two images of the same object, but with two exposures at different x-ray energies.[4] Because of the increased attenuation of the lower energy exposure, the entrance skin exposure is more than twice the exposure for a single chest radiograph. In addition, patient motion between the two exposures makes image registration complex. For this reason, one-shot techniques were developed.[5,6] These use CR plates separated by a metal filter. Both copper and tin filters were compared to determine which provided less noise (root mean square deviation) in an aluminum and plexiglas step wedge used to calibrate the system.[6] Because of their almost equivalent performance between 90 and 100 kVp, copper, 0.8 mm thick, is used in the Fuji system reported in the present article.

Previous work by the authors has compared screen/film and CR for lung nodule detection using an anthropomorphic phantom[7] and has also compared varying levels of radiation exposure when CR is used exclusively to image lung nodules embedded in varying thickness of lung simulating material.[8] The present experiments are similar, except that ES is compared to CR.

MATERIALS AND METHODS

The anthropomorphic phantom imaged by the Fuji FCR 9501 CR system was distributed by Picker (Cleveland, OH). The outer shell is muscle equivalent, whereas ribs and the spinal column are bone equivalent. Lung equivalent material fills the lung cavity, whereas more attenuating materials simulate the heart and stomach. Nodules (0.5 to 3.0 cm in diameter) were fabricated out of spackling material so that they were within 5% of lung attenuation; they were superimposed on lung tissue rather than replacing it as a lesion would. For this reason, care was taken to select only nodules which were difficult to detect. Table 1 lists their size distribution. As much as possible, nodules were placed on ribs, the peripheral lung boundaries, and in the hilar region.

The x-ray generator was manufactured by Picker (MTX). A source-to-image distance of 72 inches was maintained. Within the Fuji image receptor assembly there was a Mitaya 10:1 reciprocating grid (40 strips/cm). Plates (ST95) were loaded and

From the UCLA School of Medicine, Department of Radiological Sciences, and Department of Biomathematics, Los Angeles, CA.

Address reprint requests to Carolyn Kimme-Smith, PhD, UCLA School of Medicine, Department of Radiological Sciences, Box 951721, Los Angeles, CA 90095-1721.

0897-1889/99/1201-0004$10.00/0

Table 1. Size and Distribution of Simulated Lung Nodules

Diameter (cm)	Number of Nodules	Number of Times Used
.5	1	2
.7	1	2
.9	1	5
1.0	2	8
1.1	1	7
1.3	2	13
1.4	2	12
1.5	1	6
1.6	1	6
1.7	1	9
1.8	2	8
1.9	1	5
2.4	1	3
3.0	1	4
Total		90

processed automatically. When the ES option was selected, two CR plates were separated by a 0.8 mm copper filter. The 14 × 17 inch CR plates were read by an HeNe laser operating at 633 mm with 2.5 lp/mm spatial resolution and 10 bit gray levels.

The implementation of the ES algorithm used for the Fuji system does not require attenuation calibrations made on the x-ray equipment that are required for other implementations.[6] Of the two CR plates exposed, the front one is the low energy one, while the second one, behind the Cu filter, is the high energy image because of the attenuation of lower energy photons by the copper. The first plate can also be developed into a conventional CR image. To form the soft tissue (without bones) images tested in this work, a filter-iterative noise (FINE) algorithm was applied to the raw images from the two CR plates.[11] If Z_{hi} and Z_{lo} are the two images, then an intermediate, noisy bone image is formed from a weighted difference: $B = |Z_{hi} - Z_{lo} * W|$, where W is a weight supplied by Fuji for all ES images. After a smoothing filter with edge preservation is applied to B to form a less noisy $\hat{B}$, the final soft tissue image, S, results from subtraction: $S = |\hat{B} - \frac{1}{2}(Z_{hi} + Z_{lo})|$. Because the noise in the second image, Z_{hi}, is balanced by the less noisy Z_{lo}, the soft-tissue image should have less noise than the conventional ES algorithm, which does not average the two images. These raw images are processed by the Fuji software so that they have the usual Fuji chest radiography image enhancement processing. For the present study, a one on one format without additional edge enhancement was printed on the Fuji laser film conventionally used for CR films. Five of the soft tissue films were lighter in optical density than their comparable CR images, and so were darkened by a characteristic curve shift in the postprocessing algorithms.

Two exposures were made for each combination of nodules, both were at 100 kVp. One was at 6.4 mAs (ESE = 28.6 mR) and the second was acquired at 13 mAs (ESE = 56.7 mR). A screen/film of the same phantom required an ESE of 59.2 mR. Sensitivity or S values on CR plates represent the amount of gain or amplification needed by the photomultiplier to achieve a reasonable range of digital values. Thus images with high S values have more amplification than images with low S values and so can be expected to have more noise. S values of thoracic CR images are monitored in our clinic. A CR film is considered correctly exposed if the S number range is between 150 and 250. The average S number for the low exposure was 254 ± 15, whereas the higher exposure mean was 131 ± 12.5. Optical density (OD), mean and standard deviation, measured on the films in the lower lobe of the right lung, was 1.49 ± 0.094 for the conventional CR images, 1.20 ± .18 for the higher exposure ES images, and 1.16 ± .18 for the lower exposure ES images. Fuji changes the processing of ES images slightly to enhance contrast. While the latitude values L on conventional CR chest images is 2.2, on ES images it is 1.8. The gamma curve rotation factor is increased from 0.9 to 1.0, and the enhancement factor changes from 0.2 to 0.5 for ES images. Only five ES images were postprocessed to darken them; they were all from the higher exposure ES group and were included in the above calculations after postprocessing.

Nodules were placed on the side of the phantom closest to the image receptor to reduce image blur. Photographs of the nodules were taken for each nodule position (Fig 1). No quadrant of the film image contained more than one nodule, so the receiver operating characteristic (ROC) analysis was based on the presence or absence of a lung nodule in a quadrant of the lungs. Thus, although there were only 15 lungs without nodules in any of the four quadrants, there were an additional 62 quadrants without nodules in the 38 films containing nodules in one or more of their quadrants. There were 122 total quadrants without nodules and 90 quadrants with nodules in the 212 lung quadrants tested. Based on the photograph of the lung phantom with nodules and an associated high exposure CR image, a gold standard drawing of the nodule placement was made (Fig 2). The three image types that were compared in this study were then uniquely coded so they were keyed to the gold standard, and identifying writing on each film was obscured by black tape

Fig 1. The anthropomorphic phantom with simulated lung nodules taped to different lung quadrants.

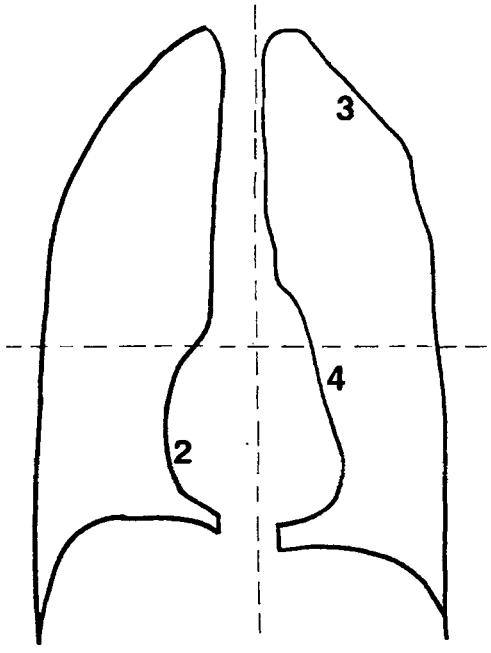

Fig 2. Gold standard drawing of the Fig 1 configuration. Note mirror image presentation. Numbers on the quadrants show nodule position and suggested ROC ratings. This image and the individual films in Fig 3 were one of four examples used for training the three radiologists before each observer session.

(Fig 3). The films for each modality were mixed so that AP (25 films) and PA (28 films) were interspersed to avoid structural noise memorization[10] and reader pattern recognition.[11] Three chest radiologists with 3, 4, and 16 years experience read each set of 53 films with at least one week separating each reading session. A supervisor was present in the same reading room for each session to repeat the instructions and present the training films. ROC grading was reviewed on the training films, with 0 assigned for a definite negative, 1 for a partial or uncertain nodule identification, 2 for possibly positive, 3 for probably positive, and 4 for definitely positive. Each reader began with a different modality to prevent presentation order bias.

An ROC analysis was used to compute the area under the ROC curve, or Az, for each reader.[12] The results were generalized to the population of chest radiologists by the jackknife method.[13] An ANOVA was then applied to the jackknife pseudovalues to investigate differences between modalities.

RESULTS

If we analyze the results as though a fixed choice test had been made, then scores of 4, 3, or 2 would indicate that a nodule was present. When we use this method, each reader identified about the same number of nodules for each modality (Table 2). By using this same method to analyze the results for peripherally located nodules, differences in the performance were only detected for the two less experienced readers (readers 1 and 2) when reading the low exposure ES images (Table 3). Only when ROC analysis was applied to the data do we obtain statistically significant differences in pooled results. The ANOVA showed that conventional CR compared to the ES soft-tissue image obtained at the same exposure was significantly better at the 98% confidence level for nodule detection (two sided $P = .048$; one sided P value = .024 (Table 4). When comparing the area under the ROC curves for the pooled data of the two ES images, obtained by using different exposures, only the one sided P test at 90% confidence level showed a significant advantage for the higher exposure images ($P = .095$) (Table 5).

DISCUSSION

There have been many experiments to show that CR is not independent of exposure, despite the wide latitude that these image receptors can tolerate.[14-16] As a result, radiologists are beginning to appreciate the emphasis that imaging scientists place on signal to noise measurements. Although CR imaging can produce a low-exposure image that looks like a chest radiograph, the diagnostic content of these images is disappointing. Previous work in energy subtraction imaging has suffered from noisy images, owing primarily to the photon deprived low-energy image resulting from higher attenuation or, for the one-shot technique, because of a noisy high energy image.[17] For the Fuji system, soft-tissue images are formed from two noisy images; even though they are smoothed and combined, poor photon flux degrades the images. By doubling the exposure, we had hoped to reduce this effect and therefore benefit from a rib-less chest radiograph. In fact, diagnosis of simulated lung nodules using the higher exposure soft-tissue image was not significantly different from diagnosis using a lower exposure conventional CR technique. Although further increases in exposure might improve the advantages of ES images, the sensitivity of the CR plates is close to its maximum using twice the conventional exposures. When CR plates are overexposed, the processing algorithm compensates for saturation by reducing the optical density. Further exposure increase may thus cause more light films that need postprocessing to achieve the correct optical density.

The manufacturer of this ES equipment does not recommend that ES images be read independently

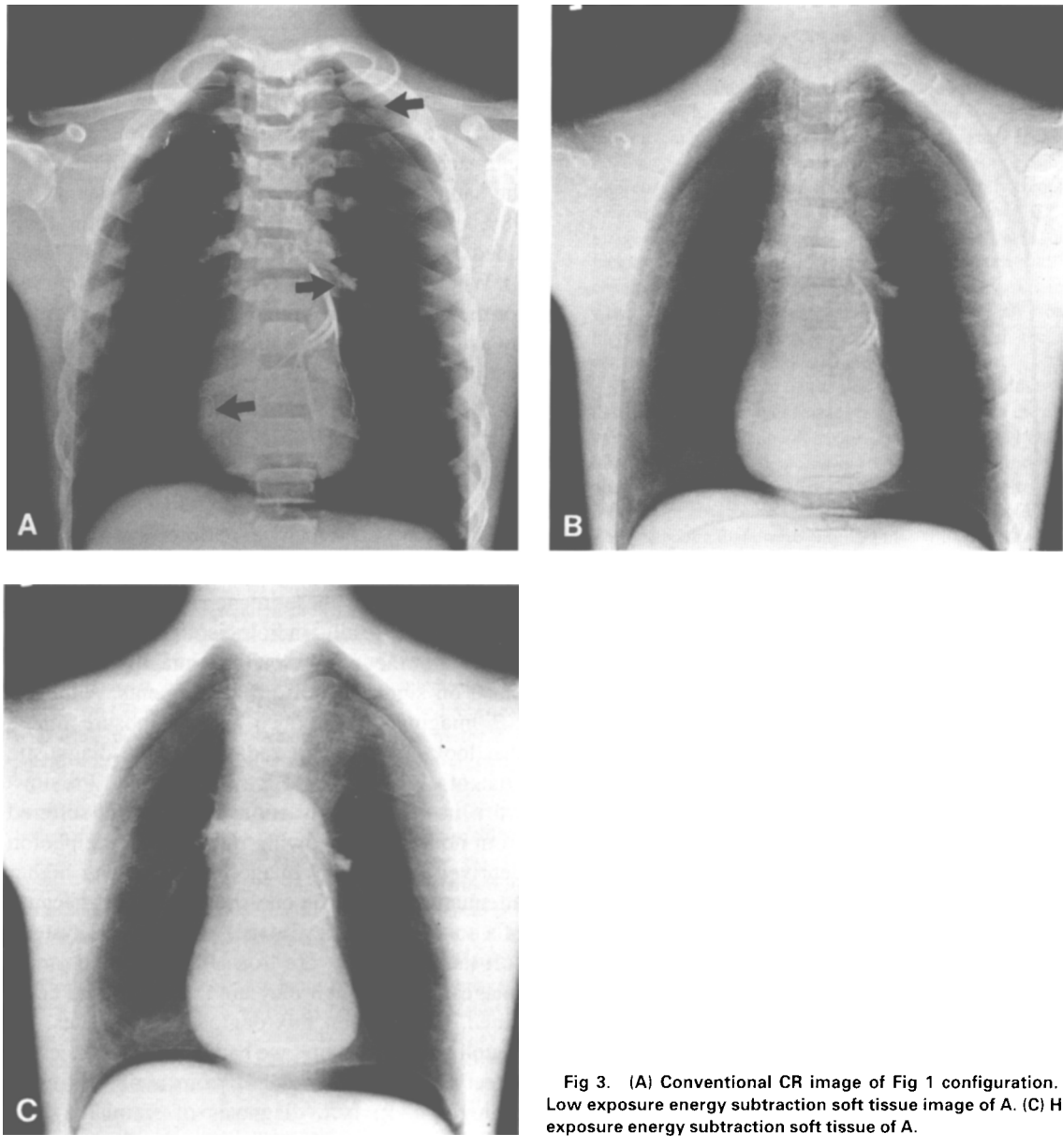

Fig 3. (A) Conventional CR image of Fig 1 configuration. (B) Low exposure energy subtraction soft tissue image of A. (C) High exposure energy subtraction soft tissue of A.

of their associated CR images. This study reinforces that recommendation. However, if obtaining a satisfactory ES image, ie, one that complements the information contained on the conventional CR image, requires twice the exposure to achieve the same diagnostic accuracy, how should ES imaging progress in the future? Can we devise combinations of images that will justify the exposure and expense of this modality? A further study, comparing the diagnostic accuracy of CR alone and ES and CR together, even if it shows improved diagnostic

Table 2. Number of Total Nodules Detected by Each Reader

Reader	Conventional CR	13 mAs ES	6.4 mAs ES	Total No. Present
1	63	64	57	90
2	62	63	60	90
3	74	75	74	90

Table 3. Number of Peripheral Nodules Detected by Each Reader

Reader	Conventional CR	13 mAs ES	6.4 mAs ES	Peripheral Nodules
1	13	14	9	25
2	13	13	9	25
3	18	18	18	25

Table 4. ROC Results for Conventional CR Versus Low mAs ES for Individual Readers and for Pooled Data

Reader	Conventional CR Az	Low mAs ES Az	95% CI	*P* Value*
1	.929	.801	−.064 to .319	.191
2	.795	.733	−.082 to .205	.399
3	.911	.840	−.027 to .169	.155
Pooled results	.878	.791	−.001 to .173	.048†

*Two sided.
†Statistically significant.

Table 5. ROC Results for Low mAs ES Versus High mAs ES for Individual Readers and for Pooled Data

Reader	Low mAs ES Az	High mAs ES Az	95% CI	*P* Value*
1	.801	.854	−.244 to .137	.583
2	.733	.766	−.173 to .107	.643
3	.836	.919	−.176 to .010	.079
Pooled results	.790	.846	−.141 to .028	.191†

*Two sided.
†Statistically significant.

accuracy, may not be a sufficient improvement to recommend the additional effort required for the combined modalities. Like many digital techniques, careful testing of their clinical capabilities must be included in the formulation of their marketing.[18]

CONCLUSION

An ROC study of a comparison of diagnostic accuracy for simulated nodule detection between conventional CR and energy subtracted soft-tissue (without ribs) images obtained at the same radiation exposure, showed that diagnostic accuracy using the conventional CR images was significantly better. A second ROC study compared the diagnostic accuracy of two soft-tissue ES images, one obtained at the conventional CR exposure and one obtained at twice that exposure. The higher exposure images were significantly better than the lower exposure images, but were not significantly better than the conventional CR images.

REFERENCES

1. MacMahon H: Digital chest radiography at the University of Chicago: Present status and future plans. J Digit Imaging 8:11-14, 1995

2. Freedman M, Stellar P, Jafroudi H, et al: Quality control of storage phosphor digital radiography systems. J Digit Imaging 8:67-74, 1995

3. Chotas HG, Floyd CE, Raven CE: Technical evaluation of a digital chest radiography system that uses a selenium detector. Radiology 195:264-270, 1995

4. Brody WR, Butt G, Hall A, et al: A method for selective tissue and bone visualization using dual energy scanned projection radiography. Med Phys 8:353-357, 1981

5. Ishigaki T, Sakuma S, Ikeda M: One-shot dual-energy subtraction chest imaging with computed radiography: Clinical evaluation of film images. Radiology 168:67-72, 1988

6. Stewart BK, Huang HK: Single-exposure dual-energy computed radiography. Med Phys 17:866-875, 1990

7. Kimme-Smith C, Aberle DR, Sayre JW, et al: Effect of reduced exposure on computed radiography: Comparison of nodule detection accuracy with conventional and asymmetric screen-film radiographs of a chest phantom. AJR Am J Roentgenol 165:269-273, 1995

8. Kimme-Smith C, Hart E, Goldin J, et al: Detection of simulated lung nodules with computed radiography: Effects of nodule size, local optical density, global object thickness, and exposure. Acad Radiol 3:735-741, 1996

9. Fuji Photo Film Co. Ltd: Fuji Computed Radiography Technical Review for FCR 9501 ES/FCR DX-A, 1996

10. Kundel HL, Revesz G: Lesion conspicuity structured noise and film reader error. AJR Am J Roentgenol 126:1233-1238, 1976

11. Metz CE: Some practical issues of experimental design and data analysis in radiological ROC studies. Invest Radiol 24:234-245, 1988

12. Dorfman DD, Alf E: Maximum likelihood estimation of parameters of signal detection theory and determination of confidence intervals: Rating method data. J Math Psychology 6:487-496, 1969

13. Dorfman DD, Berbaum KS, Metz CE: Receiver operating characteristic rating analysis: Generalization to the population of readers and patients with the jackknife method. Invest Radiol 27:723-731, 1992

14. Niklason LT, Chan HP, Cascade PN, et al: Portable chest imaging: Comparison of storage phosphor digital, asymmetric screen-film, and conventional screen film systems. Radiology 186:387-393, 1993

15. Dobbins JT, Rice JJ, Beam CA, et al: Threshold perception performance with computed and screen-film radiography: Implications for chest radiography. Radiology 183:179-187, 1992

16. Leppert AGA, Prokup M, Schaefer-Prokop CM, et al: Detection of simulated chest lesions: comparison of a conventional screen-film combination, an asymmetric screen-film system and storage phosphor radiology. Radiology 195:259-263, 1995

17. Alvarez RE, Siebert JA, Poage TF: Active dual energy x-ray detector: Experimental characterization. SPIE Med Imag 3032:419-426, 1997

18. Hendee WR, Kelsey CA, Cohen G: Point/counterpoint: Medical technologies should pass performance and cost-effectiveness review in centers of excellence before being released for diffusion in the clinical community. Med Phys 25:1099-1101, 1998